Talanta 138 (2015) 86–99

Contents lists available at ScienceDirect

Talanta

journal homepage: www.elsevier.com/locate/talanta

Standard addition method based on four-way PARAFAC decomposition to solve the matrix interferences in the determination of carbamate pesticides in lettuce using excitation–emission fluorescence data

L. Rubio [a], L.A. Sarabia [b], M.C. Ortiz [a,*]

[a] Department of Chemistry, Faculty of Sciences, University of Burgos, Plaza Misael Bañuelos s/n, 09001 Burgos, Spain
[b] Department of Mathematics and Computation, Faculty of Sciences, University of Burgos, Plaza Misael Bañuelos s/n, 09001 Burgos, Spain

ARTICLE INFO

Article history:
Received 31 October 2014
Received in revised form
26 January 2015
Accepted 31 January 2015
Available online 9 February 2015

Keywords:
Carbamate pesticides
Excitation–emission fluorescence
Parallel factor analysis
Four-way data
Iceberg lettuce
Capability of detection

ABSTRACT

The simultaneous determination of two carbamate pesticides (carbaryl and carbendazim) and of the degradation product of carbaryl (1-naphthol) in iceberg lettuce was achieved by means of PARAFAC decomposition and excitation–emission fluorescence matrices. A standard addition method for a calibration based on four-way data was applied using different dilutions of the extract from iceberg lettuce as a fourth way that provided the enough variation of the matrix to carry out the four-way analysis. A high fluorescent overlapping existed between the three analytes and the fluorophores of the matrix. The identification of two fluorescent matrix constituents through the four-way model enabled to know the matrix contribution in each dilution of the extract. This contribution was subtracted from the previous signals and a subsequent three-way analysis was carried out with the tensors corresponding to each dilution. The PARAFAC decomposition of these resulting tensors showed a CORCONDIA index equal to 99%. For the identification of the analytes, the correlation between the PARAFAC spectral loadings and the reference spectra has been used. The trueness of the method, in the concentration range studied, was guaranteed because there was neither constant nor proportional bias according to the appropriate hypothesis tests. The best recovery percentages were obtained with the data from the most diluted extract, being the results: 127.6% for carbaryl, 125.55% for carbendazim and 87.6% for 1-naphthol. When the solvent calibration was performed, the decision limit (CCα) and the capability of detection (CCβ) values, in $x_0=0$, were 2.21 and 4.38 μg L^{-1} for carbaryl, 4.87 and 9.64 μg L^{-1} for carbendazim; and 3.22 and 6.38 μg L^{-1} for 1-naphthol, respectively, for probabilities of false positive and false negative fixed at 0.05. However, these values were 5.30 and 10.49 μg L^{-1} for carbaryl, 18.05 and 35.73 μg L^{-1} for carbendazim; and 1.92 and 3.79 μg L^{-1} for 1-naphthol, respectively, when the matrix-matched calibration using the most diluted extract was carried out in the recovery study.

1. Introduction

In analytical chemistry, there is an increase in the use of higher-order data due to the current technological development [1]. The selectivity and sensitivity of the analysis are increased by the inclusion of another data dimension which provides additional information of the sample. In addition, the second-order advantage is achieved with second- (or higher-) order data and enables the accurately quantification of the calibrated analytes in the presence of non-calibrated interferents [2]. Multivariate

Abbreviations: (CCα), decision limit; (CCβ), capability of detection; (GC × GC/TOFMS), bi-dimensional gas chromatography with time of flight mass spectrometry detection; (LC × LC-DAD), bi-dimensional liquid chromatography with diode array detection; (EEM), excitation–emission fluorescence matrix; (PARAFAC), parallel factor analysis; (MCR-ALS), multivariate curve resolution-alternating least squares; (U-PLS/RTL), unfolded partial least-squares combined with residual trilinearization; (N-PLS/RTL), multi-way partial least squares combined with residual trilinearization; (AQLD), alternating quadrilinear decomposition; (AWRCQLD), alternating weighted residue constraint quadrilinear decomposition; (GC–FPD), gas chromatography coupled to flame photometric detector; (GC–μECD), gas chromatography coupled to electron capture detector; (LC–MS/MS), liquid chromatography coupled to tandem mass spectrometry; (HPLC-DAD), high-performance liquid chromatography with diode array detection; (UHPLC–MS/MS), ultra-high performance liquid chromatography coupled to tandem mass spectrometry; (UHPLC–TOF-MS), ultra-high-performance liquid chromatography/time-of-flight mass spectrometry; (IARC), International Agency for Research on Cancer; (RASFF), Rapid Alert System for Food and Feed; (MRL), maximum residue level; (IUPAC), International Union of Pure and Applied Chemistry; (LS), least squares

* Corresponding author. Tel.: +34 947 259571.
E-mail address: mcortiz@ubu.es (M.C. Ortiz).

http://dx.doi.org/10.1016/j.talanta.2015.01.042
0039-9140/

calibration models are being applied to third-order data or greater in several research fields. The calibration based on this last type of data can be named as third-order or four-way calibration; the former one is related to the number of modes of a single sample, whereas the latter focuses on the number of modes of a set of samples. So, when third-order data are joined for several samples into the fourth direction, a four-way tensor is obtained. A tutorial, in which second- and higher-order data and algorithms are reviewed, can be consulted in Ref. [3].

In the particular case of four-way data, there are different possible ways of acquiring them. By way of example, fast high-performance liquid chromatography with fluorescence excitation–emission detection for each sample can be used. In fact, several emission wavelength-elution time matrices were recorded as a function of the excitation wavelength in [4]; while four-way data were acquired by excitation–emission matrices at different elution times in [5]. Third-order data are also available by means of bi-dimensional gas or liquid chromatography (GC × GC or LC × LC, respectively) with time of flight mass spectrometry (TOFMS) or with diode array detection (DAD), such as GC × GC/TOFMS [6,7], or LC × LC-DAD [8,9].

Fluorescence spectroscopy, which is highly sensitive, can be applied to a wide range of problems in chemical and biological sciences [10]. The use of fluorescence spectroscopy also provides four-way data by introducing an additional dimension. A possible strategy is based on the recording of the excitation–emission fluorescence matrix (EEM) as a function of pH [10], volume of quencher [11] or by the measure of the time evolution of EEM data [12] while following the kinetics of a reaction. Jiménez Girón et al. [13] determined folic acid and its two main serum metabolites using four-way data which were acquired by following the photochemical reaction of these compounds by on-line UV–Vis photoirradiation. In this case, the EEMs were recorded as a function of the irradiation time.

Several third-order calibration algorithms, such as parallel factor analysis (PARAFAC) [4,5], multivariate curve resolution-alternating least squares (MCR-ALS) [5], unfolded partial least-squares and multi-way partial least squares combined with residual trilinearization (U-PLS/RTL [4,5,13], N-PLS/RTL [4,13]), alternating quadrilinear decomposition (AQLD) [14] and alternating weighted residue constraint quadrilinear decomposition (AWRCQLD) [14], among others, are available for the analysis of four-way data tensors.

The processing of second- order or higher-order data with appropriate chemometric algorithms can handle matrix interferences in complex samples [15] (olive oil samples without previous sample treatment [4], heavy fuel oil [6], environmental samples [7], milk [16], biological fluid matrices such as human plasma [10], urine [17] …). Therefore, the determination of the analytes of interest is possible even in the presence of unsuspected interferences.

The use of pesticides in agriculture is still necessary to guarantee the worldwide food supply, but a risk for both the environment and human health may be generated by their residues. Carbamate pesticides, such as carbaryl and carbendazim, are extensively used for agricultural activities. Carbaryl is used as an insecticide on corn, soybean, cotton, fruit, nut and vegetable crops, as well as in home gardens and flea treatment for pets. The mode of action of these compounds in vertebrates and insects is based on the inhibition of the activity of acetylcholinesterase enzyme in the hydrolysis of the neurotransmitter acetylcholine, which is responsible for the transmission of nervous impulses [18]. Therefore, sensitive and reliable methods for their identification and quantification in foodstuffs using all available analytical techniques should be developed to ensure food safety. In fact, the determination of carbamate pesticides can be carried out with the aid of techniques such as gas chromatography coupled to flame photometric (GC–FPD) and electron capture detectors (GC–μ ECD) [19], liquid chromatography coupled to tandem mass spectrometry (LC–MS/MS) [19,20], high-performance liquid chromatography with diode array detection (HPLC–DAD) [21], ultra-high performance liquid chromatography coupled to tandem mass spectrometry (UHPLC–MS/MS) [22] and ultra-high-performance liquid chromatography/time-of-flight mass spectrometry (UHPLC–TOF-MS) [23]. However, other works have used fluorescence spectroscopy to determine these compounds [24,25], due to their native fluorescence and to the advantages and cost of the technique. The increasing use of this technique can be shown in some reviews [26, 27]. In addition, databases of pesticides that enable to take advantage of the low cost and of the accessibility of fluorescence spectroscopy for screening are being recently developed [28].

The hydrolysis of carbaryl has been studied in several works that use four-way data [14,24,25] or even five-way data [29]. The reaction followed was the hydrolysis of carbaryl to produce 1-naphthol which is more fluorescent than carbaryl; therefore, this reaction leads to a considerable sensitivity improvement. Santa-Cruz et al. [24] and Maggio et al. [25] obtained four-way data by recording the kinetic evolution of EEM for samples containing carbaryl and 1-naphthol. The hydrolysis of propoxur was also followed in [24]. However, four-way data were acquired by following the kinetic evolution of excitation–emission phosphorescence matrices in [14]. A fourth-order multivariate calibration was proposed in [29] to process fluorescence excitation–emission-kinetic-pH data. In this last case, the hydrolysis of the analyte was followed at different pH values and the concentration of carbaryl was determined in the presence of the pesticides fuberidazole and thiabendazole as non-calibrated interferents.

The International Agency for Research on Cancer (IARC) assigned carbaryl to Group 3 (not classifiable as to its carcinogenicity to humans) in 1987. However, an IARC Advisory Group recommended that carbaryl should be given high priority for review by an IARC Monograph during 2015–2019 [30] because a significant association with melanoma has been reported by new epidemiological data and tumorigenic activity was also suggested.

The Rapid Alert System for Food and Feed (RASFF) of the European Commission has reported 2 notifications for carbaryl and 41 notifications for carbendazim from 01/10/2013 to 01/10/2014 [31]. The highest amounts of these analytes found in that period were: 35 mg kg^{-1} of carbaryl in sweet basil leaves and 54 mg kg^{-1} of carbendazim in fresh mint. These values are above the maximum residue levels (MRLs) set by regulation for these food commodities.

Since pesticide uses show significant changes over years, carbaryl and the combination of carbendazim and benomyl, among other pesticides or product combinations, should be monitored in foodstuffs according to a coordinated multiannual control programme of the European Union for 2015, 2016 and 2017 [32] to ensure compliance with MRLs and to assess the consumer exposure to pesticides residues in and on food of plant origin. By way of example, some of the products of plant origin that should be sampled in 2016 are: apples, tomatoes and lettuce. In addition, European Union has established the MRLs for carbaryl and for carbendazim in or on certain products; for example, in iceberg lettuce: 10 μg kg^{-1} for carbaryl by Commission Regulation (EU) No. 899/2012 [33] and 100 μg kg^{-1} for carbendazim by Commission Regulation (EU) No. 559/2011 [34].

As far as the authors are aware, the literature contains no reference to the determination of carbamates in lettuce by means of fluorescence data. However, the three analytes were determined using EEM fluorescence data in a different matrix (honey) [35] and the average recoveries were 148.6% for carbaryl, 102.1% for

carbendazim and 101.2% for 1-naphthol. Some recovery values are given in works that use other techniques in the analysis of carbamates in lettuce. For example, in [36], a LC–MS/MS multi-residue method was developed for the analysis of a wide range of pesticides and metabolites in fruit, vegetables and cereals. Recoveries ranged from 84 to 93% for carbaryl and from 100 to 112% for carbendazim in lettuce. Letohay et al. [37] determined pesticides by GC/MS and LC/MS/MS using QuEChERS. A 135% and 100% recovery at 250 ng g^{-1} for carbaryl were obtained by GC/MS and LC/MS/MS in lettuce, respectively and a 107% recovery was obtained for carbendazim at that concentration level in lettuce by LC/MS/MS.

In this work, the identification and quantification of two carbamate pesticides (carbaryl and carbendazim) and of the degradation product of carbaryl (1-naphthol) were carried out in a complex sample (iceberg lettuce). The simple sample treatment used was based on an extraction with ethyl acetate without adding salts and further purification was not performed. The analysis combined the use of EEM data, the standard addition method and PARAFAC. The change in the dilution of the extract in each analysis provided a four-way tensor. The signals of the three analytes were highly overlapped with each other and with the fluorescent matrix constituents and a matrix effect was also present. However, the quadrilinear PARAFAC model enabled the identification of the matrix contribution in each dilution. Then, once the contribution of the matrix fluorophores was subtracted for each dilution, a three-way analysis was carried out in solvent and in matrix-matched standards. The recovery of the method was also studied.

2. Material and methods

2.1. Chemicals

Carbaryl (CAS no. 63-25-2) and carbendazim (CAS no. 10605-21-7) (PESTANAL® grade, analytical standard), were purchased from Sigma-Aldrich (Steinheim, Germany). 1-Naphthol (CAS no. 90-15-3), methanol (CAS no. 67-56-1) (gradient grade for liquid chromatography LiChrosolv®) and ethyl acetate (CAS no. 141-78-6) (for gas chromatography SupraSolv®) were obtained from Merck KGaA (Darmstadt, Germany).

2.2. Standard solutions

Stock solutions of carbaryl, carbendazim and 1-naphthol at 400 mg L^{-1} were prepared individually in methanol and stored at 4 °C. Diluted solutions of carbaryl (2 mg L^{-1}), carbendazim (5 mg L^{-1}) and 1-naphthol (1 mg L^{-1}) were prepared from the stock solutions in the same solvent. These diluted solutions were used to prepare the solvent calibration samples in methanol at a concentration range of: 0–60 μg L^{-1} for carbaryl, 0–200 μg L^{-1} for carbendazim and 0–20 μg L^{-1} for 1-naphthol (see Table 1).

The three reference samples used for the identification of the analytes were standards, individually prepared in methanol from the diluted solutions, with concentrations of 30 μg L^{-1} of carbaryl, 100 μg L^{-1} of carbendazim and 10 μg L^{-1} of 1-naphthol.

To evaluate the recovery of the method, intermediate standard solutions of carbaryl, carbendazim and 1-naphthol were needed to prepare the spiked extracts with final concentrations of 20 μg L^{-1} of carbaryl, 80 μg L^{-1} of carbendazim and 10 μg L^{-1} of 1-naphthol. These solutions were also prepared in methanol.

2.3. Experimental procedure

2.3.1. Sample preparation method

An iceberg lettuce was purchased from a local supermarket (Burgos, Spain). This lettuce (500 g) was chopped and blended until a homogeneous mixture was obtained. Then, ten portions of the mixture were stored in a freezer. The final extract was prepared as follows: 5 g of the homogeneous sample was placed into a 50 mL polypropylene tube and 10 mL of ethyl acetate was added. The tube was shaken vigorously for 10 s by hand and stirred for another 50 s using a vortex mixer. The extract was filtered; 5 mL of the resulting filtrate was transferred into a conical glass tube and evaporated to dryness under vacuum at 40 °C using a miVac Modular Concentrator. The residue was re-dissolved in 5 mL of methanol and vortex-mixed for 60 s. This procedure was repeated and the reconstituted extracts were combined to eliminate the variability, thus the required single extract to perform the standard addition method was obtained. This final extract was collected in an amber bottle and stored under refrigeration at 4 °C. For the recovery study, the spiked extract was prepared following the procedure described above but in this case each 5 g of vegetable sample was fortified prior to extraction to contain 20 μg L^{-1} of carbaryl, 80 μg L^{-1} of carbendazim and 10 μg L^{-1} of 1-naphthol after the corresponding dilution.

Table 1
Distribution of concentrations (following a D-optimal design) for the three studied analytes used to perform the solvent calibration.

Sample	Carbaryl (μg L^{-1})	Carbendazim (μg L^{-1})	1-Naphthol (μg L^{-1})
1[a]	0	0	0
2[a]	0	0	0
3	15	0	0
4	30	0	0
5	45	0	0
6	60	0	0
7	0	50	0
8	0	100	0
9	0	150	0
10	0	200	0
11	0	0	5
12	60	100	5
13	45	150	5
14	15	200	5
15	0	0	10
16	30	50	10
17[a]	0	0	0
18	15	150	10
19	45	200	10
20	0	0	15
21	45	50	15
22	30	100	15
23	60	200	15
24	0	0	20
25	60	50	20
26	15	100	20
27	30	150	20
28[b]	15	200	20
29[b]	30	100	15
30[b]	60	200	5
31[b]	15	0	10
32[b]	45	50	0
33[b]	0	100	10
34[a]	0	0	0

[a] Methanol blank.
[b] Samples for validation.

2.3.2. Standard addition samples

The matrix-matched standards were prepared by adding a fixed volume of the final extract (2.5 mL, 1.5 mL or 0.5 mL, depending on the required dilution in each stage of this work), the appropriate volume of the solutions (diluted solutions mentioned in Section 2.2) of each analyte into 5 mL volumetric flasks and completed to the mark with methanol, so that, the desired concentration of every analyte was achieved for each experiment.

For the recovery study, the corresponding spiked final extract for each dilution was used to prepare these samples.

2.4. Instrumental

A vortex stirrer LBX Instruments V05 series (Barcelona, Spain), with speed control, was used. The Whatman™ glass microfiber filters (GF/C grade, 90 mm diameter, 1.2 μm) were obtained from GE Healthcare (Little Chalfont, UK). A miVac Modular Concentrator (GeneVac Limited, Ipswich, UK) which consisted of a miVac Duo concentrator, a SpeedTrap™ (condenser) and a Quattro pump was used for evaporation of the solvent.

Fluorescence measurements were performed at room temperature on a PerkinElmer LS 50B Luminescence Spectrometer (Waltham, MA, USA) equipped with a xenon discharge lamp. In all cases, a 10 mm quartz SUPRASIL® cell with cell volume of 3.5 mL by Perkin Elmer (Waltham, MA, USA) was used. The corresponding excitation–emission matrices were recorded in the following ranges: emission (295–500 nm, each 1 nm) when the excitation wavelengths vary from 240 to 290 nm (each 5 nm). Excitation and emission monochromator slit-widths were both set to 10 nm. The scan speed was 1500 nm min^{-1}.

2.5. Software

The D-optimal experimental design was built with NEMRODW [38]. The FL WinLab software (PerkinElmer) was used to register the fluorescent signals. The data were imported to Matlab using the INCA software [39] that inserts missing values into the matrix in the wavelengths that correspond to the Rayleigh effect. The PLS_Toolbox 6.0.1 [40] for use with Matlab [41] was employed for PARAFAC calculations. STATGRAPHICS [42] was used for building and validating the linear regressions. Decision limit (CCα) and capability of detection (CCβ) were calculated with DETARCHI [43] and CCα and CCβ [44] at the maximum residue level were estimated using NWAYDET (a program written in-house that evaluates the probabilities of false non-compliance and false compliance for n-way data).

3. Theory

3.1. Four-way PARAFAC decomposition

Fluorescence spectroscopy is by far the most abundant type of data used for multi-way analysis due to the close relationship between the PARAFAC model and the fundamental structure of common fluorescence spectroscopic data, as Bro stated in [45].

The quadrilinear PARAFAC model for a four-way tensor $\underline{\mathbf{X}}$ with dimension $(I \times J \times K \times L)$ which contains the fluorescence intensity of sample i-th at the excitation wavelength k-th, emission wavelength j-th and l-th level of dilution, is:

$$x(i,j,k,l) = \sum_{f=1}^{F} a_{if} b_{jf} c_{kf} d_{lf} + \varepsilon_{ijkl}, \quad i = 1,\ldots,I, \quad j = 1,\ldots,J, \quad k = 1,\ldots,K, \quad l = 1,\ldots,L \tag{1}$$

When there are F fluorophores in the samples and a tensor of experimental data is compatible with the structure of Eq. (1); that is, the data are quadrilinear, the PARAFAC model of F components (number of factors) can be used to estimate: (i) the extinction coefficients for each analyte at all wavelengths (i.e. the excitation profile or excitation spectrum) by means of the loading vector $\mathbf{c}_f=(c_{1f}, c_{2f},\ldots,c_{Kf})$; (ii) the relative emission at all wavelengths (i.e. the emission profile or emission spectrum of each analyte) by means of $\mathbf{b}_f=(b_{1f}, b_{2f},\ldots,b_{Jf})$; (iii) the relative concentration of every analyte in all the samples (i.e. the sample profile) by means of the vector $\mathbf{a}_f=(a_{1f}, a_{2f},\ldots,a_{If})$ and (iv) the fluorescence quantum yield (i.e. the dilution profile in this work) by means of $\mathbf{d}_f=(d_{1f}, d_{2f},\ldots, d_{Lf})$. This last fourth mode could also be the time, quenching, pH, etc., profiles depending on the experimental data used. Finally, ε_{ijkl} is the residue that is not fitted by the model. The vectors $\mathbf{b}_f$, $\mathbf{c}_f$ and $\mathbf{d}_f$ are normalized to unit length to avoid trivially different solutions (Eq. (1)) in which the vectors $\boldsymbol{a_f}$, $\boldsymbol{b_f}$, $\boldsymbol{c_f}$ and $\boldsymbol{d_f}$ would differ from each other by a constant factor, for example $3\boldsymbol{b_f}$ and $(1/3)\boldsymbol{c_f}$. Therefore, three of these vectors that are usually the last ones of the data tensor are normalized to unit length. The coordinates of the four loading vectors ($\mathbf{a}_f$, $\mathbf{b}_f$, $\mathbf{c}_f$ and $\mathbf{d}_f$) are contained in the loading matrices $\mathbf{A}$ (dimension $I \times F$), $\mathbf{B}$ (dimension $J \times F$), $\mathbf{C}$ (dimension $K \times F$) and $\mathbf{D}$ (dimension $L \times F$).

However, if a tensor $\underline{\mathbf{X}}$ with dimension $(I \times J \times K)$ is used, the fourth mode (related to the vector $\mathbf{d}_f$) is not considered in the PARAFAC decomposition. Therefore, when the fluorescence intensities are arranged as a three-way tensor, the trilinear PARAFAC model is:

$$x(i,j,k) = \sum_{f=1}^{F} a_{if} b_{jf} c_{kf} + \varepsilon_{ijk}, \quad i = 1,\ldots,I, \quad j = 1,\ldots,J, \quad k = 1,\ldots,K \tag{2}$$

The elements of the three loading vectors ($\mathbf{a}_f$, $\mathbf{b}_f$, $\mathbf{c}_f$) for each factor in Eq. (2) have the same meaning as in Eq. (1). So, the quadrilinear PARAFAC model is a direct extension of its trilinear model.

When experimental data correspond to models (1) and (2), the PARAFAC decomposition provides unique profile estimations [46]. In chemical analysis, the determination of analytes in the presence of uncalibrated interferents is known as the second order advantage. The uniqueness property of the PARAFAC model ensures this advantage.

The PARAFAC model is found by minimizing the sum of squares of the residuals. Alternating least squares (ALS) is an algorithm widely used for fitting the PARAFAC model although other algorithms may be used [47]. The ALS algorithm handles higher-order data and constrained models.

The core consistency diagnostic (CORCONDIA), which is an index that measures the degree of trilinearity of the experimental data tensor, was developed by Bro and Kiers [48]. This index assesses the similarity between the imposed superdiagonal tensor $\underline{\mathbf{T}}$ of ones of the PARAFAC model and the least squares-fitted core tensor $\underline{\mathbf{G}}$, which is formed by the loading vectors of PARAFAC obtained from a Tucker3 model:

$$\text{CORCONDIA} = 100\left(1 - \frac{\sum_{p=1}^{F}\sum_{q=1}^{F}\sum_{r=1}^{F}\left(g_{pqr} - t_{pqr}\right)^2}{\sum_{p=1}^{F}\sum_{q=1}^{F}\sum_{r=1}^{F}\left(t_{pqr}\right)^2}\right) \tag{3}$$

where g_{pqr} are the elements of tensor $\underline{\mathbf{G}}$ (the fitted Tucker3 core), t_{pqr} are the elements of tensor $\underline{\mathbf{T}}$ and F is the number of factors in the model.

CORCONDIA is always less than or equal to 100% and may also be negative. A CORCONDIA close to 100% implies an appropriate model. However, this index is not used as the only measure for the validity of the model; for example, the coherence of the loadings with the experimental knowledge should be also taken into account.

The indices Q and Hotelling's T^2 explain how well a model is describing a given sample. The Q residual index indicates the difference or residual between the value of the sample and its projection on the subspace of the model. The models of

Eqs. (1) and (2) can be written as $\underline{\mathbf{X}} = \underline{\hat{\mathbf{X}}} + \underline{\mathbf{E}}$. As a result, the residuals are contained in the tensor $\underline{\mathbf{E}}$, that can be divided into a tensor $\underline{\mathbf{E}}_i$ (Eq. (1)) or into a matrix $\mathbf{E}_i$ (Eq. (2)) for each one of the samples $i=1,\ldots,I$. The sum of squares can be calculated from these tensors (matrices) yielding a vector of I values $\mathbf{s}_I = (s_1, \ldots, s_I)$. The value s_i corresponding to the i-th sample can be tested using the distributional properties of the residual data. The critical value Q_α for the residuals at a confidence level $1-\alpha$ is calculated [49] from all the residuals using the moments of first, θ_1, second, θ_2, and third order, θ_3:

$$Q_\alpha = \theta_1 \left[\frac{z_\alpha \sqrt{2\theta_2 h_0^2}}{\theta_1} + \frac{\theta_2 h_0 (h_0 - 1)}{\theta_1^2} + 1 \right]^{1/h_0} \quad (4)$$

where $h_0 = 1 - 2\theta_1\theta_3/3\theta_2^2$ and z_α is the normal deviate cutting off an area of α under the upper tail of the distribution if h_0 is positive and under the lower tail if h_0 is negative. Values of s_i higher than Q_α are an indication that the i-th sample cannot be adequately represented by the PARAFAC model.

A sample is influential in the PARAFAC model if its Mahalanobis distance to the center of data is large. The index for the i-th sample, that is proportional to that distance, is defined as the i-th element of the following vector [50]:

$$T^2 = I \times \mathrm{diag}\left[\mathbf{A} \left(\mathbf{A}^{\mathrm{T}} \mathbf{A} \right)^{-1} \mathbf{A}^{\mathrm{T}} \right] \quad (5)$$

where $\mathbf{A}$ is the PARAFAC matrix of loadings for the sample profile. The T^2 for each sample is compared with the critical value at the confidence level $1-\alpha$:

$$T_\alpha^2 = \frac{F(I-1)}{I-F} F_{F,I-F,\alpha} \quad (6)$$

where F and I are the same as in Eqs. (1) or (2). $F_{F,I-F,\alpha}$ is the critical value at α of a F distribution with F and $I-F$ degrees of freedom.

T^2 can be considered the counterpart to Q residuals. Taken together, these two statistics give how much variance the model captured (T^2) and how much was left over (Q). These statistics are used to identify outlier samples in every way. So, when both indices exceed the threshold value at a certain confidence level in a sample, the PARAFAC model should be estimated again without that sample.

3.2. Decision limit and capability of detection

According to the ISO norm 11843 [51], the decision limit is "the value of the net concentration the exceeding of which leads, for a given error probability α, to the decision that the concentration of the analyte in the analyzed material is larger than that in the blank material". Decision 2002/657/EC [52] accepts this definition as CCα or decision limit. Whereas the capability of detection or minimum detectable net concentration has been defined, for a given probability of false positive α, as "the true net concentration of the analyte in the material to be analyzed which will lead, with probability $1-\beta$, to the correct conclusion that the concentration in the analyzed material is different from that in the blank material". This definition has also been accepted by the International Union of Pure and Applied Chemistry (IUPAC) [53]. The minimum detectable net concentration is named CCβ in [52], whereas in the ISO standard 11843 is x_d.

However, the definition provided by the ISO 11843 [51] for the capability of detection leaves outside analytical procedures based on multivariate calibrations, despite the excellent results obtained with them even in the presence of interferents, overlapping signals, etc. A procedure to apply the methodology of the ISO 11843 [51] to multivariate or multi-way analysis was proposed in [54,44], respectively. The generalization is based on the mathematical proof [54] that the capability of detection is not modified by linear transformations of the response (the signal). As a consequence, the same capability of detection is obtained using the regression "calculated concentration" versus "true concentration". Once the regression model has been validated, a Neyman–Pearson test (unilateral case) is applied.

In that test, the null hypothesis (H_0) states that there is not analyte in the sample ($x_0=0$) and the alternative hypothesis (H_A): there is analyte in the sample ($x_0 > 0$). The decision depends on a α value (probability of false positive, probability of rejecting H_0 when is true) and a β value (probability of false negative, probability of accepting H_0 when is false).

The capability of detection can be estimated using the following equation:

$$\mathrm{CC}\beta = \frac{\Delta(\alpha,\beta)\omega_{x_0}\hat{\sigma}}{\hat{b}} \quad (7)$$

where Δ is the parameter of a non-central Student's t-distribution, ω_{x_0} is a function of the standard concentrations, $\hat{\sigma}$ and $\hat{b}$ are the residual standard deviation and the slope of the regression "calculated concentration" versus "true concentration", respectively.

On the other hand, [52] also defines the capability of detection in the case of substances with an established permitted limit. This means that the detection capability is the concentration at which the method is able to detect permitted limit concentrations with a statistical certainty of $1-\beta$. The permitted limit is "the maximum residue limit, maximum level or other maximum tolerance for substances established elsewhere in Community legislation". The capability of detection at the MRL will be estimated with x_0=MRL and α and β are the probabilities of false non-compliance and of false compliance, respectively.

4. Results and discussion

4.1. Reference spectra for the identification of the analytes

In every stage of this work, the identification of each analyte was carried out through the correlation between its emission and excitation reference spectra and the emission and excitation loadings estimated from the corresponding PARAFAC model, respectively. The unequivocal identification of the analytes using the reference spectra is required by the legislation currently in force.

The experimental spectra were obtained from the EEMs of the pure analytes. So, standards prepared in methanol, whose composition is described in Section 2.2, were measured. Fig. 1 shows the EEM landscapes and contour plots of these samples. As can be seen in this figure, the carbendazim and carbaryl spectra are highly overlapped; especially in the excitation range from 270 to 290 nm and in the emission range from 300 to 350 nm. In addition, it is clear that both spectra are also overlapped from the emission wavelength 300 to 400 nm with the spectrum of 1-naphthol. The order of the fluorescence intensity of the signals is: 1-naphthol > carbaryl > carbendazim. In this work, the maximum fluorescence intensity in excitation spectra appears at 280, 275 and 240 nm for carbendazim, carbaryl and 1-naphthol, respectively. Carbendazim has an emission maximum in the recorded region at 310 nm, carbaryl at 334 nm and 1-naphthol at 355 nm. The excitation and emission spectra at the wavelengths of maximum emission and excitation were taken, respectively, for each analyte. These excitation and emission reference spectra are represented by continuous lines in Fig. 2(a) for carbaryl, in Fig. 2(b) for carbendazim and in Fig. 2(c) for 1-naphthol. The graphs corresponding to the emission are on the left and the

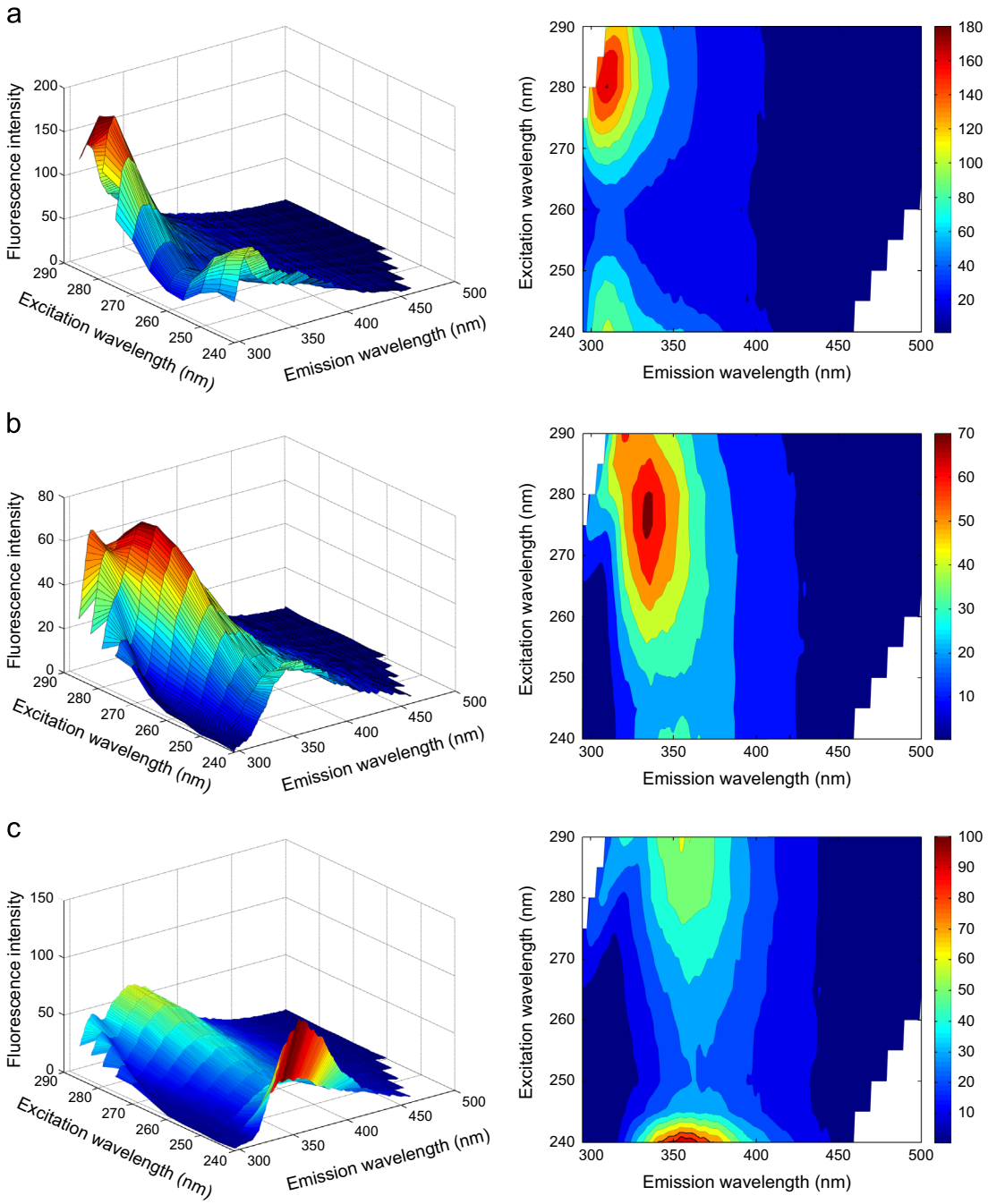

Fig. 1. EEM landscapes (left-hand side figures) and contour plots (right-hand side figures) for each pure analyte in methanol: (a) 100 μg L^{-1} of carbendazim, (b) 30 μg L^{-1} of carbaryl and (c) 10 μg L^{-1} of 1-naphthol.

excitation ones are placed on the right in Fig. 2. It must be noticed that the values have been normalized in this figure to compare them with the spectra obtained in next stages of this work.

4.2. Solvent calibration

First, the analysis was performed in synthetic samples, using pure methanol as solvent. The distribution of concentrations for the three analytes to carry out the solvent calibration was chosen following the experimental plan of a D-optimal design which enabled to reduce the experimental effort. The concentration range was: 0–60 μg L^{-1} for carbaryl, 0–200 μg L^{-1} for carbendazim and 0–20 μg L^{-1} for 1-naphthol and each analyte was at five levels of concentration. Therefore, the number of experiments required for the performance of the initial factorial design would be $5^3=125$ experiences. Four pure standards of increasing concentrations for each analyte were proposed as protected points of the design; in Table 1 these 12 samples were: samples number 3 to 6 for carbaryl, samples 7 to 10 for carbendazim and samples 11, 15, 20 and 24 for 1-naphthol. A methanol blank (sample number 2) was also a protected point of the design. Thus, a 25-experiment D-optimal design was selected so the experimental effort was reduced by 80%. The 12 remaining samples selected were ternary mixtures (samples 12 to 14, 16, 18, 19, 21 to 23, 25 to 27 of Table 1). In addition, another 3 ternary mixtures (samples 28 to 30 of Table 1) and 3 binary mixtures (samples 31 to 33 of Table 1) were measured for validation. Three methanol blanks (samples 1, 17 and 34 of Table 1) were also measured throughout the experimentation to

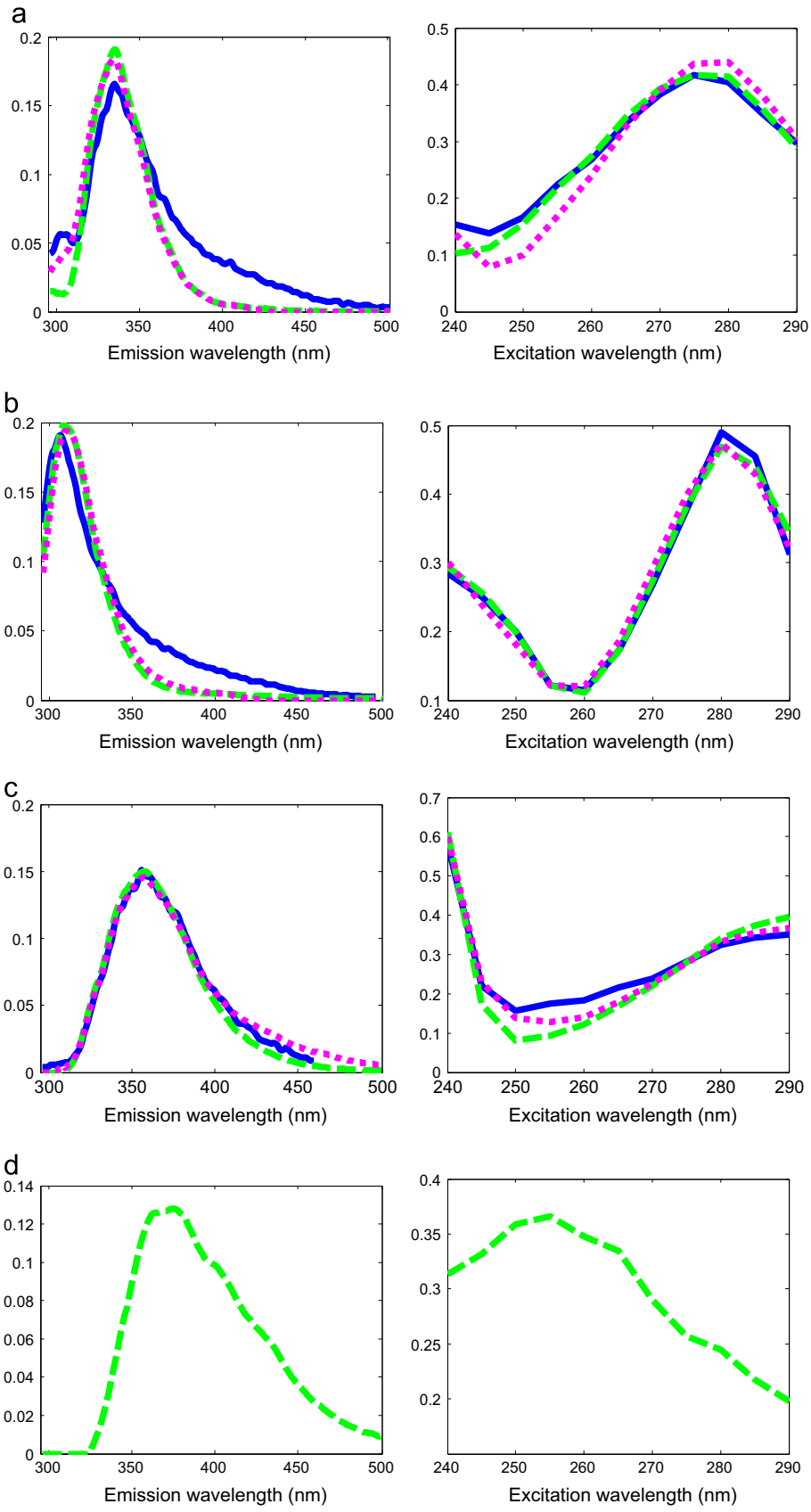

Fig. 2. Comparison between the excitation and emission reference spectra and the excitation and emission loadings of the PARAFAC models obtained in the solvent calibration stage (Section 4.2) and in the recovery study (Section 4.3.1) for: (a) carbaryl, (b) carbendazim, (c) 1-naphthol and (d) the background. Emission: left-hand side figures, excitation: right-hand side figures. The reference spectra are represented by dark blue continuous line, the loadings of the four-factor model obtained in the solvent calibration step are represented by light green dashed line and the ones obtained in the three-factor model of the recovery step are represented by pink dotted line. (For interpretation of the references to color in this figure legend, the reader is referred to the web version of the article).

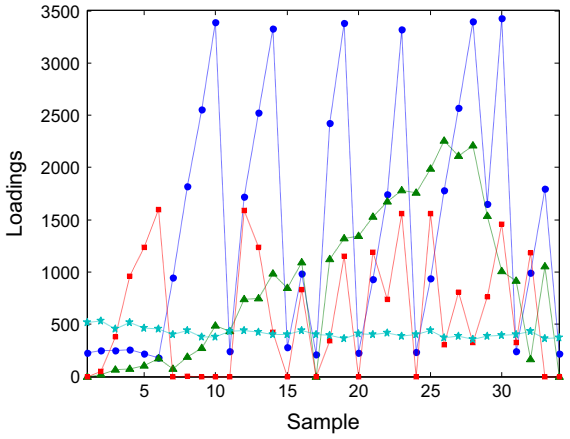

Fig. 3. Loadings of the sample profile of the four-factor PARAFAC model fitted with the data tensor $\underline{\mathbf{X}}_1$. Factor 1 (carbendazim): blue dots, factor 2 (1-naphthol): green triangles, factor 3 (carbaryl): red squares, factor 4 (background): cyan stars. (For interpretation of the references to color in this figure legend, the reader is referred to the web version of the article).

assure the absence of experimental drift. Table 1 shows the concentration of the different calibration samples prepared in methanol.

The EEM matrices of all these samples were arranged, in the order shown in Table 1, to constitute the tensor $\underline{\mathbf{X}}_1$ ($34 \times 206 \times 11$). The first dimension of this tensor refers to the number of samples, the second corresponds to the number of emission wavelengths and the third is the number of excitation wavelengths recorded. The PARAFAC decomposition has been applied to this tensor with the non-negativity constraint imposed for the three ways, as both the excitation and emission spectra must always be positive. A four-factor PARAFAC model was chosen (CORCONDIA of 93% and explained variance of 99.84%). The outlier data diagnostic is performed through Q and Hotelling's T^2 indices. At the confidence level of 95%, no outlier data were detected. The first three factors represent carbendazim, 1-naphthol and carbaryl, respectively. The correlation coefficients for the excitation and emission profiles, regarding the reference spectra, were 0.994 and 0.977 for carbendazim, 0.986 and 0.996 for 1-naphthol and 0.995 and 0.964 for carbaryl, respectively. The fourth factor is the background. The loadings of the sample mode of these four factors are included in Fig. 3, whereas the dashed lines in Fig. 2(a) for carbaryl, Fig. 2 (b) for carbendazim, Fig. 2(c) for 1-naphthol and Fig. 2(d) for the background show the excitation loadings (graphs on the right) and emission loadings (graphs on the left). The three factors related to the analytes follow the expected pattern in the sample mode and the sample loadings for the background (represented by cyan stars) remain constant (see Fig. 3).

For each analyte, a LS regression between the sample loadings and the true concentration was built with all the samples except for the six validation samples. The fourth sample in the calibration line for carbaryl had a standardized residual greater than 2.5 in absolute value, so it was considered an outlier and removed. A new LS fitting was performed and validated with the remaining data for carbaryl. In all cases, the regression models were significant and there was not lack of fit at a 99% confidence level. Table 2 shows the parameters of the calibration lines estimated for each analyte, and other figures of merit. According to ISO 5725, the term accuracy includes trueness and precision [55]. The accuracy is verified, in a concentration range, with the regression "calculated concentration versus true concentration" that assesses the trueness of the method using the hypothesis tests (for the slope and for the intercept) and evaluates the precision by the residual sum of squares of that regression. As a result, this regression is named "accuracy line". Table 2 shows the parameters of the accuracy line obtained for each analyte.

The mean of the absolute value of the relative errors are also listed in Table 2. These values ranged from 2.73% to 10.62% in calibration and from 3.17% to 9.28% in prediction when the samples with calculated concentrations lower than the capability of detection (CCβ) have been excluded. The lowest values were obtained for carbendazim. The property of trueness was verified for all the analytes; that is, the intercept is 0 and the slope is 1 at the 95% confidence level. The lowest values for the decision limit, CCα, (for a probability of false positive (α) fixed at 0.05) and for the capability of detection (being the probabilities of false positive and false negative (β) equal to 0.05) were obtained for carbaryl; while the highest values were obtained for carbendazim (see Table 2).

4.3. Quantification and identification in an iceberg lettuce sample

In this section, the standard addition method has been proposed to determine the three analytes in the iceberg lettuce sample. Initial studies were carried out to select the adequate dilution of the extract from lettuce and it was concluded that the extract should be diluted twice at least to perform the analysis. The extract was prepared following the experimental procedure described in Section 2.3.1. The distribution of concentrations chosen was the same as in Section 4.1, but the concentrations of carbaryl were reduced by a third and the ones for carbendazim were reduced by a 20% with regard to Table 1. Therefore, the levels of concentration were: 0, 10, 20, 30 and 40 μg L^{-1} for carbaryl, 0, 40, 80, 120 and 160 μg L^{-1} for carbendazim and 0, 5, 10, 15 and 20 μg L^{-1} for 1-naphthol. The test sample (sample number 2 of Table 3) and three replicates of this sample were measured (samples number 1, 17 and 34 of Table 3). As in the previous section, three methanol blanks were measured throughout the experimentation to assure the absence of experimental drift but they were not included in the analysis (samples not shown in Table 3). In this case, the matrix-matched standards were prepared with the extract two times diluted and following the procedure described in Section 2.3.2. Table 3 shows only the concentrations of the 34 matrix-matched samples of this standard addition method.

The tensor $\underline{\mathbf{X}}_2$ ($34 \times 206 \times 11$), which contains the EEM matrices placed in the order of Table 3, was built. The coherence of the PARAFAC model with the experimental knowledge was taken into account to determine the appropriate number of factors. None of the PARAFAC models estimated from this tensor were totally coherent. For example, the factors associated to carbendazim and 1-naphthol were coherent in the five-factor model (factor 1–3: the three analytes, factor 4: background, factor 5: matrix; CORCONDIA < 0) but there was a confusion between the loadings of carbaryl and the loadings of the matrix. Therefore, the matrix contribution and carbaryl were not well-separated in this model. In addition, all the sample loadings of carbendazim were very high, even the ones of the samples that did not contain this analyte. This fact may be due to a matrix effect, which will lead to a wrong estimation of the concentration of the analyte in the sample. On the other hand, the six-factor PARAFAC model was less coherent than this last one.

The EEM landscape of the extract diluted twice (see Fig. 4(a)) shows that the iceberg lettuce matrix is fluorescent in the same region as the analytes (see Fig. 1). Therefore, the existence of a high fluorescent overlapping, as can be seen in Fig. 4(b), makes the determination of the analytes in that complex extract difficult. The highest variation in the fluorescent intensity is around 150 in this standard addition method (see Fig. 4(a) and (b)).

With the aim of quantifying the three analytes in the complex sample, a four-way analysis was proposed. So, the same standard

Table 2
Parameters of the regression line "sample loading versus true concentration (C_{true})" and accuracy line for carbaryl, carbendazim and 1-naphthol for the solvent calibration stage. Decision limit (CCα) and capability of detection (CCβ) at $x_0=0$. Probabilities of false positive (α) and false negative (β) fixed at 0.05.

		Carbaryl	Carbendazim	1-Naphthol
Calibration line	Slope, b_1	26.40	15.51	95.26
	Intercept, b_0	−1.51	218.61	147.08
	Residual standard deviation, s_{yx}	33.09	42.82	173.92
	Correlation coefficient, ρ	0.999	0.999	0.974
	Number of outliers removed	1 (Sample 4)	–	–
	$\overline{\lvert e_r \rvert}_{calibration}$ [a]	5.17 ($n=15$)	2.73 ($n=16$)	10.62 [b] ($n=12$)
	$\overline{\lvert e_r \rvert}_{prediction}$ [a]	9.28 ($n=5$)	3.17 ($n=5$)	8.80 [b] ($n=4$)
Accuracy line	Slope, b_1	0.999	1	1
	Intercept, b_0	1.36×10^{-4}	5.86×10^{-6}	-1.59×10^{-10}
	Residual standard deviation, s_{yx}	1.25	2.76	1.82
	Decision limit, CCα ($x_0=0$) (μg L^{-1})	2.21	4.87	3.22
	Capability of detection, CCβ [c] ($x_0=0$) (μg L^{-1})	4.38	9.64	6.38

[a] $\overline{\lvert e_r \rvert}$ is the mean of the absolute value of the relative error.
[b] Samples with calculated concentration lower than the capability of detection were excluded.
[c] $\alpha=\beta=0.05$.

Table 3
Distribution of concentrations (following a D-optimal design) of the three analytes in the matrix-matched standards to perform the standard addition method.

Sample	Carbaryl (μg L^{-1})	Carbendazim (μg L^{-1})	1-Naphthol (μg L^{-1})
1 [a]	0	0	0
2 [a]	0	0	0
3	10	0	0
4	20	0	0
5	30	0	0
6	40	0	0
7	0	40	0
8	0	80	0
9	0	120	0
10	0	160	0
11	0	0	5
12	40	80	5
13	30	120	5
14	10	160	5
15	0	0	10
16	20	40	10
17 [a]	0	0	0
18	10	120	10
19	30	160	10
20	0	0	15
21	30	40	15
22	20	80	15
23	40	160	15
24	0	0	20
25	40	40	20
26	10	80	20
27	20	120	20
28 [b]	10	160	20
29 [b]	20	80	15
30 [b]	40	160	5
31 [b]	10	0	10
32 [b]	30	40	0
33 [b]	0	80	10
34 [a]	0	0	0

[a] Test sample.
[b] Samples for validation.

addition method was performed at other two different dilutions of the extract (1.5 mL and 0.5 mL of the extract added to 5 mL volumetric flasks). The corresponding matrix-matched standards were prepared following the procedure described in Section 2.3.2.

First, a three-way analysis was carried out for the two new experimental data sets. The dimensions of these two data tensors $\underline{\mathbf{X_3}}$ and $\underline{\mathbf{X_4}}$ which were built from the data of the analyses performed with 1.5 mL and 0.5 mL of the extract, respectively, were ($34\times206\times11$). Six factors were necessary in the PARAFAC decomposition of both three-way tensors. In these PARAFAC models (CORCONDIA < 0), three factors were unequivocally identified as the three analytes, other two factors were linked to two fluorophores present in the iceberg lettuce matrix and the last factor was associated with the background. The sample loadings for carbaryl and carbendazim were still very high for all the samples in the model obtained with $\underline{\mathbf{X_3}}$, but the values were lower than the ones obtained in the five-factor model of the tensor $\underline{\mathbf{X_2}}$. However, in the case of the standard addition method performed with the extract ten times diluted, the sample loadings of the three analytes were very low compared to the two previous cases, even some of them were close to zero for the samples that did not contain these analytes. So, the results of the PARAFAC decomposition improved when the dilution of the extract was higher; that is, when the matrix effect was reduced. In [56], a mathematical proof is given to explain why a data tensor cannot be trilinear when a standard addition method is used with three-way EEM data.

Therefore, according to these conclusions and taking into account that the best results were obtained with a too high dilution, a four-way analysis of the data was carried out. So, the three-way tensors that contained the data of the same standard addition performed at three different dilutions of the extract ($\underline{\mathbf{X_2}}$, $\underline{\mathbf{X_3}}$ and $\underline{\mathbf{X_4}}$ for the first, second and third dilutions, respectively) were arranged to provide a four-way tensor $\underline{\mathbf{X_5}}$ with dimension ($34\times206\times11\times3$). Thus, the fourth mode is the level of dilution of the extract. The non-negativity constraint was imposed for the four ways. The PARAFAC model needed six factors, with explained variance of 99.96% and no outlier data were found. The six factors were the same as in the three-way models obtained for $\underline{\mathbf{X_3}}$ and $\underline{\mathbf{X_4}}$: two of the factors corresponded to the fluorescent lettuce matrix constituents, another factor was related to the background and the rest were unequivocally identified as the three analytes. In all cases, the correlation coefficients for the three analytes were greater than 0.97 for the excitation and emission profiles when these are compared with the reference spectra. The representation of the loadings of each mode is shown in Fig. 5. The sample mode is common to all the dilutions due to the use of a four-way model. The sample loadings followed the expected pattern for the analytes and remained constant for the rest of the components, as Fig. 5(a) shows. In addition, these sample loadings were low compared to the ones obtained in the three-way models except for carbendazim, but the variation between the lowest and the highest value for this analyte was greater than in the previous cases. Therefore, the estimated concentration for this analyte will be lower than before. The degree of difficulty in determining the analytes is clearly shown through the spectral profiles (see Fig. 5 (b)) which were highly overlapped. In fact, the emission spectrum

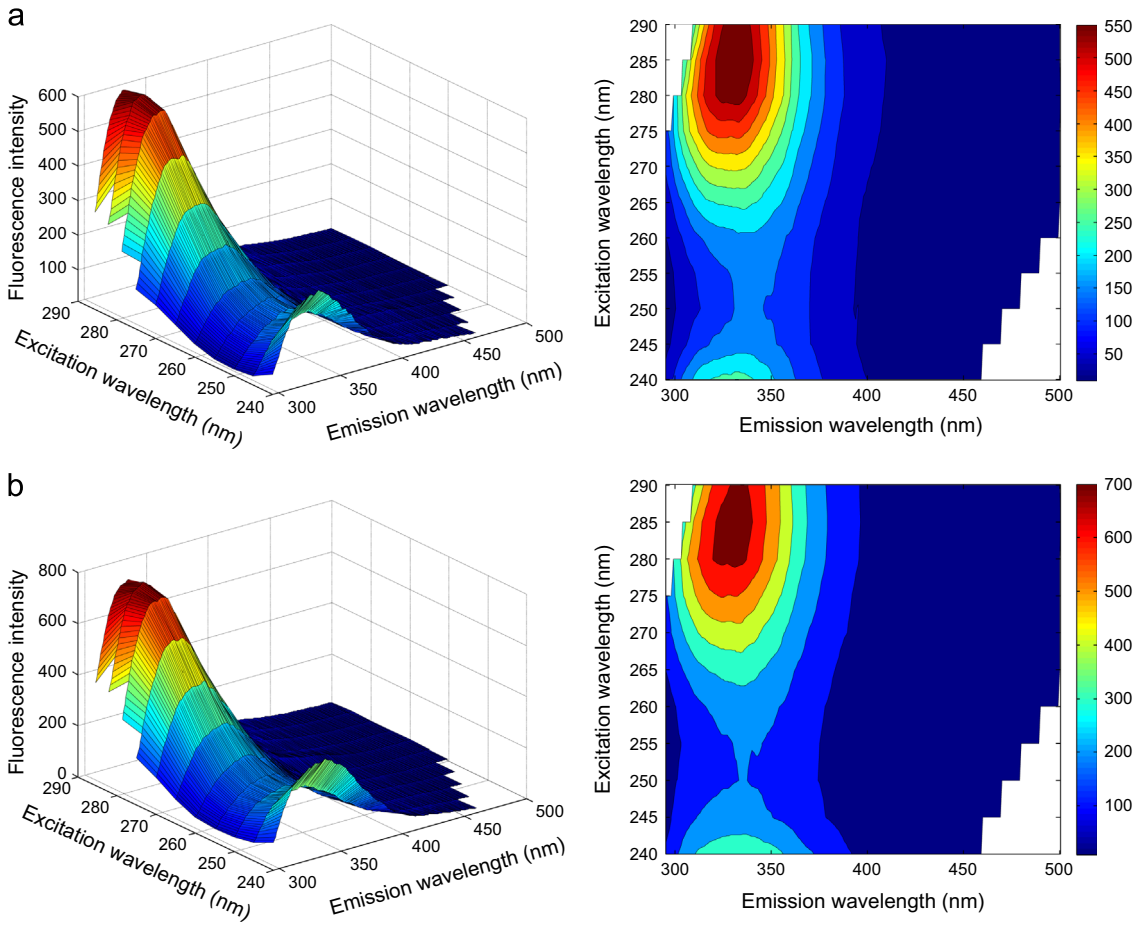

Fig. 4. EEM landscapes (left-hand side figures) and contour plots (right-hand side figures) of: (a) the lettuce matrix diluted twice, (b) extract two times diluted with a concentration of 40 μg L^{-1} of carbaryl, 160 μg L^{-1} of carbendazim and 15 μg L^{-1} of 1-naphthol.

of carbaryl was totally overlapped with the one of a fluorescent matrix constituent. This would explain why it was so difficult to obtain a valid model. The dilution mode (see Fig. 5(d)) was also coherent: the loadings of the three analytes and the background remained nearly constant in the three extract dilutions; while the loadings of the two fluorophores of the matrix decreased from the first to the third dilution, that is, the lowest values were obtained for the most diluted extract.

However, the CORCONDIA value of this model was less than zero. This means that the uniqueness of the solution reached is not assessed. The "ad hoc" procedure used in [56] to recover the trilinearity was followed in this work. This strategy is based on subtracting the contribution of the factors which are not associated to the analytes from the original data tensor. The normalized excitation–emission matrices obtained through the tensor product of the spectral loadings of each factor can be seen in Fig. 6(a) and (b) for the two matrix fluorophores and the one for the background is shown in Fig. 6(c). But, due to the use of a four-way model in this work, the tensor product of each normalized matrix and of each loading of the dilution mode was applied for the factors that are not related to the analytes. Then, the resultant matrices for each dilution were multiplied by the sample loading of the measured samples of the corresponding factor to obtain these matrices in real units of fluorescent intensity. These final matrices were concatenated to form a data tensor in each case. Thus, a data tensor was obtained for each dilution and for each factor. For each dilution, the tensors obtained for the three factors were taken away from the original data tensor of that dilution. Therefore, these final data tensors only contain the contribution of the analytes. A four-way tensor, $\underline{\underline{\mathbf{X}}}_{6}$, was built with those three final tensors. When the PARAFAC decomposition of that four-way tensor was performed, a three-factor model resulted where the loadings were nearly the same as the ones of the previous four-way model. But, the CORCONDIA value was still less than zero because the quantities of the analytes were the same in each dilution due to the use of the same standard addition scheme for the three extract dilutions. In consequence, the data tensor is not quadrilinear. The variation in the concentrations of the analytes in each dilution was not enough to recover the CORCONDIA using the procedure explained above. As Ref. [56] proved, the CORCONDIA index should increase when the factors that remain nearly constant are removed from the tensor.

According to these conclusions, a new strategy was proposed. In the measured samples for each dilution, the amounts of the analytes vary, while the matrix and background remain constant. So, the CORCONDIA index should increase if the three-way PARAFAC decomposition is carried out with the three-way tensors of each dilution that only contain the contribution of the analytes. These data tensors are the ones contained in the four-way tensor $\underline{\underline{\mathbf{X}}}_{6}$. Therefore, the contribution of the matrix fluorophores and of the background in each dilution was obtained through the loadings of the quadrilinear model and taken away from the original data tensor of its corresponding dilution. Thus, a three-way analysis can be performed. The PARAFAC decomposition of those three data tensors resulted in three-factor models, with no outliers samples detected. In all cases, the three analytes were unequivocally identified and the correlation coefficients for the excitation and emission profiles are collected in the third and fourth column

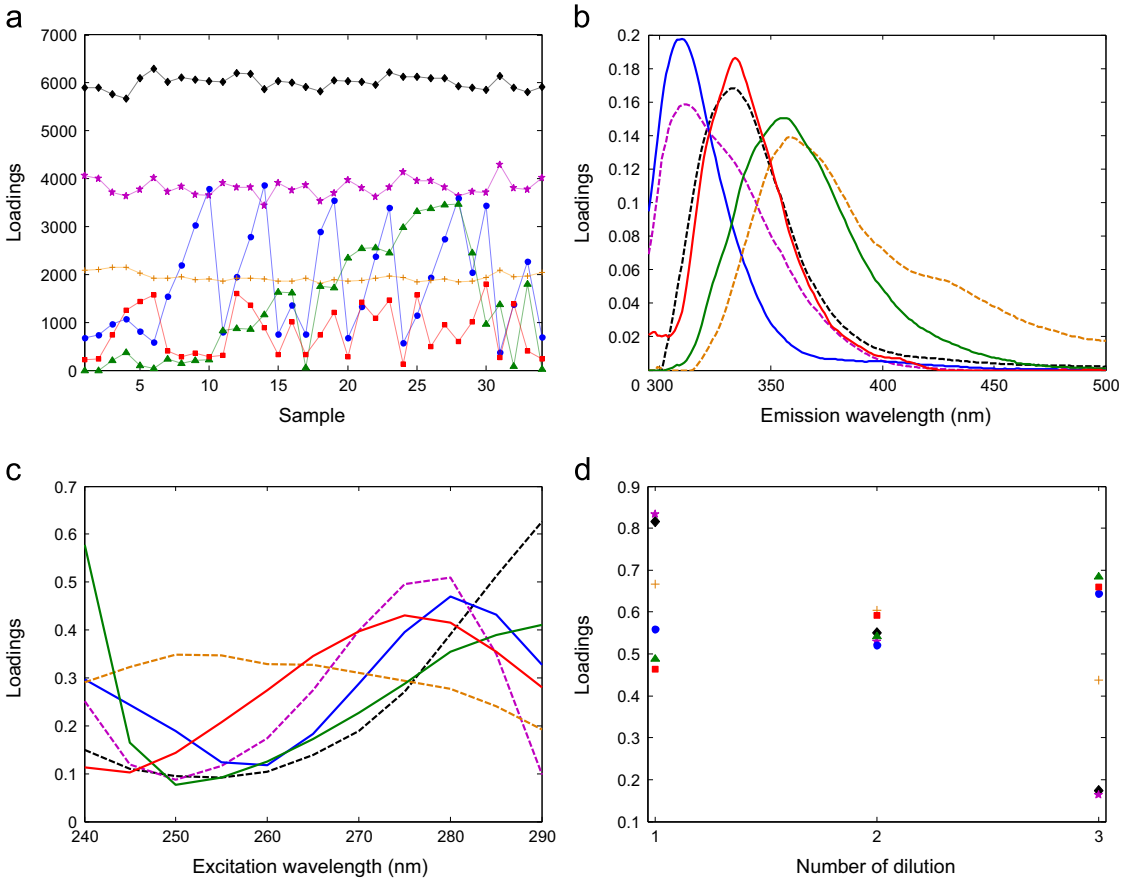

Fig. 5. Loadings of the four-way PARAFAC model with six factors obtained with the data tensor $\underline{\mathbf{X}}_5$ ($34 \times 206 \times 11 \times 3$) for the: (a) sample mode, (b) emission mode, (c) excitation mode and (d) dilution mode. Carbendazim is in blue, carbaryl in red, 1-naphthol in green, two fluorophores of the iceberg lettuce matrix in purple and black, and the background in orange. In the sample and dilution mode, carbendazim is also represented by dots, carbaryl by squares, 1-naphthol by triangles, the background by crosses and the two fluorophores of the matrix by rhombus and stars. In the emission and excitation mode, the three analytes are represented by continuous lines and the rest of the components by dashed lines. (For interpretation of the references to color in this figure legend, the reader is referred to the web version of the article).

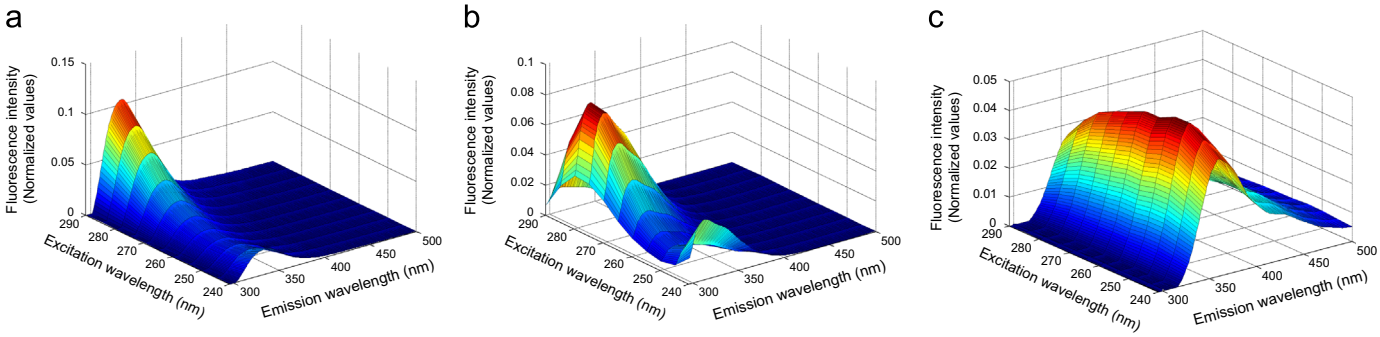

Fig. 6. EEM landscapes (normalized) built through the tensor product of the spectral loadings obtained in the four-way PARAFAC decomposition of the factors associated with: (a) and (b) two fluorophores present in the iceberg lettuce matrix and (c) the background.

of Table 4, respectively. The CORCONDIA index was equal to 99% in those three PARAFAC models, so this procedure has enabled the recovery of the trilinearity.

The calibration lines "sample loading versus added concentration" were performed for each analyte and for the three cases. The three replicates of the test sample (samples number 1, 17 and 34 of Table 3) and the six validation samples (samples number 28 to 33 of Table 3) formed the test set and the rest of the samples were used as calibration set (25 mixture samples). The results of the LS regressions obtained for each analyte in each case are shown in Table 4. The regressions were significant in all cases and there was not lack of fit at a 95% confidence level. Some outliers were detected (see the eighth column of Table 4), so they were removed and a new LS regression was performed and validated with the remaining data (fifth column of Table 4). The mean of the absolute value of the relative errors, both in calibration (from 4.70% to 12.98%) and in prediction (from 4.55% to 11.41%), also figures on the last columns of this table. In all cases, the values for carbaryl were calculated considering only the samples with concentrations higher than CCβ. The accuracy line was used to calculate the figures of merit, which are shown in Table 5. The trueness of the method was verified for all the analytes at a 95% confidence level. The values of CCα (for α=0.05) and CCβ (for probabilities of false positive and false negative fixed at 0.05) for every analyte were determined (see fifth and seventh columns of Table 5). The values for carbaryl and carbendazim were higher than those obtained in the solvent calibration (Section 4.2, Table 2), which is

Table 4
Correlation coefficients between the reference spectra and the excitation-emission profiles and results of the regression "sample loading versus added concentration" for carbaryl, carbendazim and 1-naphthol obtained with the three-factor models estimated from the PARAFAC decomposition of the tensors containing the data from each standard addition method performed at three different dilutions of the iceberg lettuce extract. The parameters "s_{yx}" and "ρ" are the standard deviation and the correlation coefficient of the regression, respectively.

Case of study	Analyte	Correlation coefficient		Calibration line					
		Excitation	Emission	Model	ρ	s_{yx}	Outliers	$\overline{\lvert e_r \rvert}_{\text{calibration}}$ [a]	$\overline{\lvert e_r \rvert}_{\text{prediction}}$ [a]
1st Dilution	Carbaryl	0.997	0.968	$y=15.91x+96.59$	0.976	58.04	2 (Samples 4, 14)	8.40[b] ($n=11$)	7.16[b] ($n=3$)
	Carbendazim	0.993	0.978	$y=9.62x+464.60$	0.983	111.13	–	12.98 ($n=16$)	4.55 ($n=5$)
	1-Naphthol	0.964	0.991	$y=78.23x+66.28$	0.996	52.60	1 (Sample 24)	5.09 ($n=15$)	5.75 ($n=5$)
2nd Dilution	Carbaryl	0.998	0.977	$y=18.41x+239.41$	0.976	66.77	2 (Samples 4, 14)	8.32[b] ($n=11$)	8.65[b] ($n=3$)
	Carbendazim	0.994	0.979	$y=9.57x+314.51$	0.991	77.70	1 (Sample 14)	8.80 ($n=15$)	5.95 ($n=5$)
	1-Naphthol	0.955	0.992	$y=86.37x+42.02$	0.996	57.59	–	5.72 ($n=16$)	4.97 ($n=5$)
3rd Dilution	Carbaryl	0.998	0.965	$y=22.18x+171.33$	0.976	77.57	1 (Sample 4)	10.83[b] ($n=11$)	11.33[b] ($n=3$)
	Carbendazim	0.991	0.984	$y=11.81x+458.47$	0.987	118.28	–	12.10 ($n=16$)	10.36 ($n=5$)
	1-Naphthol	0.979	0.994	$y=107.12x+97.82$	0.997	67.60	3 (Samples 4, 14, 24)	4.70 ($n=14$)	11.41 ($n=5$)

[a] $\overline{\lvert e_r \rvert}$ is the mean of the absolute value of the relative error.
[b] Samples with calculated concentration lower than the capability of detection were excluded.

Table 5
Parameters of the accuracy line together with some validation parameters for carbaryl, carbendazim and 1-naphthol obtained with the three-factor models estimated from the PARAFAC decomposition of the tensors containing the data from each standard addition method performed at three different dilutions of the iceberg lettuce extract. Concentration of the three analytes in the sample and the confidence interval in each case.

Case of study	Analyte	Accuracy line		CCα ($\mu g\ L^{-1}$)		CCβ ($\mu g\ L^{-1}$)[a]		Sample concentration	
		Model	s_{yx}	($x=0$)	($x=$MRL)[b]	($x=0$)	($x=$MRL)[b]	($\mu g\ L^{-1}$)	Interval (at 95% confidence level)
1st Dilution	Carbaryl	$y=0.99x+3.40\times10^{-5}$	3.65	6.56	16.44	12.98	22.74	6.07	(−1.81, 14.42)
	Carbendazim	$y=0.99x-1.49\times10^{-5}$	11.56	20.66	120.4	40.89	140.3	48.30	(22.97, 75.12)
	1-Naphthol	$y=1.02x-5.90\times10^{-2}$	0.55	0.99	–	1.91	–	0.85	(−0.60, 2.32)
2nd Dilution	Carbaryl	$y=1.00x+2.64\times10^{-5}$	3.63	6.52	16.40	12.88	22.65	13.00	(5.01, 21.60)
	Carbendazim	$y=0.99x+3.48\times10^{-5}$	8.12	14.54	114.4	28.79	128.5	32.86	(15.11, 51.30)
	1-Naphthol	$y=1.00x-1.65\times10^{-6}$	0.67	1.91	–	2.36	–	0.49	(−0.94, 1.94)
3rd Dilution	Carbaryl	$y=1.00x-9.42\times10^{-6}$	3.50	6.26	16.15	12.38	22.16	7.72	(0.16, 15.74)
	Carbendazim	$y=1.00x+3.63\times10^{-5}$	10.02	17.89	117.6	35.41	134.9	38.82	(16.96, 61.65)
	1-Naphthol	$y=0.99x-2.44\times10^{-5}$	0.63	1.14	–	2.26	–	0.91	(−0.46, 2.32)

[a] $\alpha=\beta=0.05$.
[b] MRL: 10 $\mu g\ L^{-1}$ for carbaryl and 100 $\mu g\ L^{-1}$ for carbendazim.

mainly due to a lower residual standard deviation of the accuracy line for both analytes in the solvent calibration. However, the values for 1-naphthol were lower than the ones obtained in Section 4.2 because the highest value of the residual standard deviation for this analyte was obtained in the solvent calibration. These figures of merit were also estimated at the MRL established in [33,34] for carbaryl (10 $\mu g\ L^{-1}$) and for carbendazim (100 $\mu g\ L^{-1}$) in iceberg lettuce for probabilities of false non-compliance (α) and false compliance (β) equal to 0.05 (see sixth and eighth columns of Table 5).

Taking the use of the standard addition method into account in this work, the concentration of the three analytes in the iceberg lettuce sample was obtained through the calibration line. The amounts found for each analyte together with the corresponding confidence interval are listed in the two last columns of Table 5 for each case. When the values of concentration for each analyte were compared, it is concluded that the results are quite similar in all cases. The analyte 1-naphthol was not detected in the sample because the confidence interval at a 95% confidence level contained zero in all cases and the found concentration values were lower than the decision limit. In addition, the values obtained for carbaryl and carbendazim were below the corresponding CCβ (or very close, in the case of carbendazim). One confidence interval for carbaryl also contained zero. So, it could be concluded that none of the analytes were detected in the sample above the MRL.

The four-way PARAFAC decomposition together with the procedure followed to recover the trilinearity have provided successful results in contrast with the impossibility of performing a three-way analysis. Therefore, the use of a fourth way (the variation of the matrix) in the PARAFAC decomposition has allowed the separation of the matrix contribution.

To sum up, the steps to follow for analyzing a new test sample should be: first, three different dilutions of the extract obtained from the test sample are taken and the same standard addition method is performed with each of them. Then, a four-way tensor is built with the recorded data. The PARAFAC decomposition of that tensor is performed and the contribution of the factors related to the matrix is removed from the original data. Finally, a three-way PARAFAC analysis is carried out. Therefore, although this procedure needs a considerable number of samples (pure analytes, binary and ternary mixtures), the time required to record all those samples is less than in a chromatographic analysis due to the use of fluorescence spectroscopy. In fact, each sample is measured in about 3 min.

In addition, the control of the measurement procedure is guaranteed through the three different dilution measures. This allows to assess the precision in the determination of the test sample.

4.3.1. Recovery study

To evaluate the recovery of the three analytes from the iceberg lettuce matrix, the strategy described in Section 4.3 was followed. So, a four-way tensor ($\underline{\mathbf{X}}_7$) was built with the data from the standard addition method performed at the same three different dilutions of the extract. This time, the extract used to carry out the analysis was spiked with the three analytes at the beginning of the

procedure (see Section 2.3.1). It was necessary to prepare three spiked extracts since the concentration of the three analytes should be the same in all cases after the corresponding dilution to carry out a four-way analysis. So, the lettuce sample was spiked to contain a concentration of the analytes after each dilution equal to the concentration corresponding to the central level of the D-optimal design (20 μg L^{-1} of carbaryl, 80 μg L^{-1} of carbendazim and 10 μg L^{-1} of 1-naphthol). Once the corresponding extract was obtained, the matrix-matched standards were prepared as Section 2.3.2 described. In this case, the concentrations of each analyte added to the spiked extract to obtain each standard were the same as in Section 4.3 (see Table 3) except for the six samples for validation which were not included this time. In addition, two more replicates of the test sample (5 replicates of the test sample in total) were also measured throughout the experimentation.

The data were arranged to provide the four-way tensor, $\underline{\mathbf{X}}_7$, with dimension $(30 \times 206 \times 11 \times 3)$. The PARAFAC model of this tensor needed six factors with a CORCONDIA value less than zero again, as expected. These factors were the same as those obtained in the four-way PARAFAC decomposition of the tensor $\underline{\mathbf{X}}_6$ (Section 4.3): the three analytes, two fluorescent matrix components and the background. No outlier data were found at a 99% confidence level and the loadings of the four modes were coherent with the experimental knowledge. The correlation coefficient for 1-napthol between the excitation profile and the reference spectrum (see the third column of Table 6) improved regarding the values obtained in the previous section.

With the aim of recovering the trilinearity, the strategy used in Section 4.3 was followed; that is, the contribution of the matrix fluorophores and of the background obtained through the loadings of the four-way model of six factors of $\underline{\mathbf{X}}_7$ was subtracted from the original three-way tensor of each dilution. But, this procedure was now only applied to the tensor of the third dilution because the matrix contribution is expected to be less when the most diluted extract is used. In addition, the use of a four-way PARAFAC model allows the selection of that high dilution for the analysis because the effect of the dilution is collected in the fourth mode and the sample profile is common to all the dilutions. Fig. 7 clearly shows the difference between the sample loadings of the two fluorescent matrix components for each dilution of the extract. These values have been obtained through the three-factor PARAFAC models of the tensors of each dilution in which there is only the contribution of those two compounds and the background. As can be seen in this figure, the sample loadings for the matrix are so high for the first dilution (the least diluted extract) and they decrease from the first to the third dilution, as expected. The sample loadings of the analytes were much lower than the ones of the matrix for the first and second dilution; whereas the sample loadings of the matrix were below the ones of the analytes in the last dilution. Therefore, the lowest matrix/analyte ratio was obtained in the third dilution, so the results obtained with that dilution should be the best. Thus, a PARAFAC model of three factors (CORCONDIA of 99%, explained variance of 99.66%) was chosen for the data tensor that only contained the contribution of the analytes in the third dilution. The spectral loadings of this model are compared with the corresponding reference spectra in Fig. 2.

The calibration lines and the corresponding accuracy lines for each analyte were computed. All the samples were used as calibration set (except for the five replicates of the test sample), that is, 25 samples in total. The results obtained in both cases are collected in Table 6. The property of trueness was fulfilled in all cases by the analytical method. The values of CCα and CCβ for carbaryl were better than those obtained in the previous matrix-matched calibration (Section 4.3), while the values for 1-naphthol were even better than those achieved in the solvent calibration (see Table 2).

The recovery rates were estimated for each analyte, being the results: 127.6% for carbaryl, 125.55% for carbendazim and 87.6% for 1-naphthol with the data from the third dilution. So, the best results were obtained for 1-naphthol, which may be caused by a lower spectral overlapping compared to the other analytes.

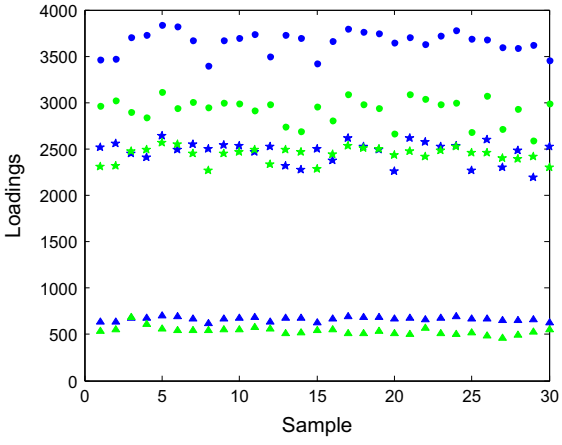

Fig. 7. Sample loadings of the two fluorescent components present in the iceberg lettuce matrix for each dilution: first dilution, in dots; second dilution, in stars and third dilution, in triangles. For each case, one matrix fluorophore is in dark blue, while the other one is in light green. (For interpretation of the references to color in this figure legend, the reader is referred to the web version of the article).

Table 6
Correlation coefficients between the excitation and emission profiles and the reference spectra and parameters of the regression "sample loading versus added concentration" and of the accuracy line for carbaryl, carbendazim and 1-naphthol obtained, in the recovery study step (Section 4.3.1), with the three-factor model estimated from the PARAFAC decomposition of the tensor containing the data from the standard addition method performed with the most diluted extract of the iceberg lettuce. Parameters: s_{yx} is the standard deviation; ρ is the correlation coefficient of the regression.

Analyte	Correlation coefficient		Calibration line		Accuracy line	CCα (μg L^{-1})		CCβ (μg L^{-1})[f]	
	Exc[a]	Em[b]	Model; (ρ; s_{yx}; outliers)	$\overline{\lvert e_r \rvert}_{\text{calibration}}$[c]	Model; (s_{yx})	($x=0$)	($x=$MRL)[e]	($x=0$)	($x=$MRL)[e]
Carbaryl	0.990	0.961	$y=25.13x+641.15$; (0.982; 74.60; –)	5.65[d] ($n=12$)	$y=1.00x-1.14\times10^{-5}$; (2.97)	5.30	15.20	10.49	20.30
Carbendazim	0.991	0.986	$y=11.09x+1114.28$; (0.987; 112.14; –)	14.66 ($n=16$)	$y=1.00x+1.46\times10^{-9}$; (10.11)	18.05	117.80	35.73	135.20
1-Naphthol	0.993	0.997	$y=83.76x+733.42$; (0.988; 89.24; sample 27, 28, 29)	8.43 ($n=13$)	$y=1.00x-5.97\times10^{-6}$; (1.06)	1.92	–	3.79	–

[a] Exc: correlation coefficient for the excitation profile.
[b] Em: correlation coefficient for the emission profile.
[c] $\overline{\lvert e_r \rvert}$ is the mean of the absolute value of the relative error.
[d] Samples with calculated concentration lower than the capability of detection were excluded.
[e] MRL: 10 μg L^{-1} for carbaryl and 100 μg L^{-1} for carbendazim.
[f] $\alpha=\beta=0.05$.

5. Conclusions

The four-way PARAFAC decomposition applied to EEM fluorescence signals, together with the use of the standard addition method and the proposed strategy to recover the trilinearity, made it possible to quantify and identify carbaryl, carbendazim and 1-naphthol unequivocally in the iceberg lettuce matrix despite the high overlapping signals and the presence of other fluorophores. The variation of the matrix, which was achieved through the use of different dilutions of the extract in the analysis, has provided a fourth way in the PARAFAC decomposition. The efficiency of the four-way PARAFAC analysis with these data has been demonstrated in this work despite the fact that the fluorescent signal of the lettuce matrix was highly overlapped with the analytes. The four-way analysis was needed to obtain the matrix contribution in each dilution through the loadings of the model in a satisfactory way. In a subsequent three-way analysis, the most diluted extract provided the best results. Separating the contribution of the matrix from that of the analytes in the original signal guarantees the correct performance of the standard addition method. This fact would have been impossible using zero-order data whereas it would be only possible with first- or second-order data in some special cases. None of the analytes were detected above the MRL in the analyzed lettuce.

Acknowledgements

The authors thank the financial support provided by projects of the Ministerio de Economía y Competitividad (CTQ2011-26022) and Junta de Castilla y León (BU108A11-2). L. Rubio is particularly grateful to Universidad de Burgos for her FPI grant.

References

[1] P.M. Kroonenberg, Applied Multiway Analysis, John Wiley & Sons, Inc., New Jersey, 2008.
[2] A.C. Olivieri, Anal. Chem. 80 (2008) 5713–5720.
[3] G.M. Escandar, H.C. Goicoechea, A. Muñoz de la Peña, A.C. Olivieri, Anal. Chim. Acta 806 (2014) 8–26.
[4] V.A. Lozano, A. Muñoz de la Peña, I. Durán-Merás, A. Espinosa Mansilla, G.M. Escandar, Chemom. Intell. Lab. Syst. 125 (2013) 121–131.
[5] M.R. Alcaráz, G.G. Siano, M.J. Culzoni, A. Muñoz de la Peña, H.C. Goicoechea, Anal. Chim. Acta 809 (2014) 37–46.
[6] H. Parastar, J.R. Radovi, M. Jalali-Heravi, S. Diez, J. Maria Bayona, R. Tauler, Anal. Chem. 83 (2011) 9289–9297.
[7] A.E. Sinha, C.G. Fraga, B.J. Prazen, R.E. Synovec, J. Chromatogr. A 1027 (2004) 269–277.
[8] S.E.G. Porter, D.R. Stoll, S.C. Rutan, P.W. Carr, J.D. Cohen, Anal. Chem. 78 (2006) 5559–5569.
[9] H.P. Bailey, S.C. Rutan, Chemom. Intell. Lab. Syst. 106 (2011) 131–141.
[10] C. Kang, H.-L. Wu, L.-X. Xie, S.-X. Xiang, R.-Q. Yu, Talanta 122 (2014) 293–301.
[11] N. Rodríguez, M.C. Ortiz, L.A. Sarabia, Talanta 77 (2009) 1129–1136.
[12] A. Muñoz de la Peña, I. Durán Merás, A. Jiménez Girón, H.C. Goicoechea, Talanta 72 (2007) 1261–1268.
[13] A. Jiménez Girón, I. Durán-Merás, A. Espinosa-Mansilla, A. Muñoz de la Peña, F. Cañada Cañada, A.C. Olivieri, Anal. Chim. Acta 622 (2008) 94–103.
[14] X.-D. Qing, H.-L. Wu, X.-F. Yan, Y. Li, L.-Q. Ouyang, C.-C. Nie, R.-Q. Yu, Chemom. Intell. Lab. Syst. 132 (2014) 8–17.
[15] K. Calimag-Williams, G. Knobel, H.C. Goicoechea, A.D. Campiglia, Anal. Chim. Acta 811 (2014) 60–69.
[16] N. Rodríguez, M.C. Ortiz, L.A. Sarabia, Anal. Chim. Acta 651 (2009) 149–158.
[17] M.C. Ortiz, L.A. Sarabia, M.S. Sánchez, D. Giménez, Anal. Chim. Acta 642 (2009) 193–205.
[18] A. Ruiz-Medina, E.J. Llorent-Martínez, M.L. Fernández-de Córdova, P. Ortega-Barrales, J. Food Compos. Anal. 26 (2012) 66–71.
[19] A. Nunes Oliveira Jardim, D. Carvalho Mello, F. Caroline Silva Goes, E. Ferreira Frota Junior, E. Dutra Caldas, Food Chem. 164 (2014) 195–204.
[20] K.M. Kasiotis, C. Anagnostopoulos, P. Anastasiadou, K. Machera, Sci. Total Environ. 485–486 (2014) 633–642.
[21] V. Boeris, J.A. Arancibia, A.C. Olivieri, Anal. Chim. Acta 814 (2014) 23–30.
[22] D. Moreno-González, J.F. Huertas-Pérez, A.M. García-Campaña, L. Gámiz-Gracia, Talanta 128 (2014) 299–304.
[23] P. Sivaperumal, P. Anand, L. Riddhi, Food Chem. 168 (2015) 356–365.
[24] P. Santa-Cruz, A. García-Reiriz, Talanta 128 (2014) 450–459.
[25] R.M. Maggio, P.C. Damiani, A.C. Olivieri, Anal. Chim. Acta 677 (2010) 97–107.
[26] Á. Andrade-Eiroa, M. Canle, V. Cerdá, Appl. Spectrosc. Rev. 48 (2013) 1–49.
[27] Á. Andrade-Eiroa, M. Canle, V. Cerdá, Appl. Spectrosc. Rev. 48 (2013) 77–141.
[28] S. Foudeil, H. Hassoun, T. Lamhasni, S. Ait Lyazidi, F. Benyaich, M. Haddad, M. Choukrad, A. Boughdad, M. Bounakhla, H. Bounouira, R.M.B.O. Duarte, A. Cachada, A.C. Duarte, Environ. Sci. Pollut. Res. (2014), http://dx.doi.org/10.1007/s11356-014-3807-6.
[29] R.M. Maggio, A. Muñoz de la Peña, A.C. Olivieri, Chemom. Intell. Lab. Syst. 109 (2011) 178–185.
[30] World Health Organization and International Agency for Research on Cancer (WHO/IARC), IARC Monographs on the Evaluation of Carcinogenic Risks to Humans (INTERNAL REPORT 14/002). Report of the Advisory Group to Recommend Priorities for IARC Monographs during 2015–2019, Lyon (France), 2014.
[31] RASFF Portal. See: ⟨https://webgate.ec.europa.eu/rasff-window/portal/index.cfm⟩ (accessed 30/10/2014).
[32] Commission Implementing Regulation (EU) No 400/2014 of 22 April 2014 Concerning a Coordinated Multiannual Control Programme of the Union for 2015, 2016 and 2017 to Ensure Compliance with Maximum Residue Levels of Pesticides and to Assess the Consumer Exposure to Pesticide Residues in and on Food of Plant and Animal Origin, Off. J. Eur. Union L 119:44–56.
[33] Commission Regulation (EU) No 899/2012 of 21 September 2012 Amending Annexes II and III to Regulation (EC) No 396/2005 of the European Parliament and of the Council as Regards Maximum Residue Levels for Acephate, Alachlor, Anilazine, Azocyclotin, Benfuracarb, Butylate, Captafol, Carbaryl, Carbofuran, Carbosulfan, Chlorfenapyr, Chlorthal-dimethyl, Chlorthiamid, Cyhexatin, Diazinon, Dichlobenil, Dicofol, Dimethipin, Diniconazole, Disulfoton, Fenitrothion, Flufenzin, Furathiocarb, Hexaconazole, Lactofen, Mepronil, Methamidophos, Methoprene, Monocrotophos, Monuron, Oxycarboxin, Oxydemeton-methyl, Parathion-methyl, Phorate, Phosalone, Procymidone, Profenofos, Propachlor, Quinclorac, Quintozene, Tolylfluanid, Trichlorfon, Tridemorph and Trifluralin in or on Certain Products and Amending that Regulation by Establishing Annex V Listing Default Values, Off. J. Eur. Union L 273:1–75.
[34] Commission Regulation (EU) No 559/2011 of 7 June 2011 Amending Annexes II and III to Regulation (EC) No 396/2005 of the European Parliament and of the Council as Regards Maximum Residue Levels for Captan, Carbendazim, Cyromazine, Ethephon, Fenamiphos, Thiophanate-methyl, Triasulfuron and Triticonazole in or on Certain Products, Off. J. Eur. Union L 152:1–21.
[35] S.-H. Zhu, H.-L. Wu, B.-R. Li, A.-L. Xia, Q.-J. Han, Y. Zhang, Y.-C. Bian, R.-Q. Yu, Anal. Chim. Acta 619 (2008) 165–172.
[36] M. Hiemstra, A. de Kok, J. Chromatogr. A 1154 (2007) 3–25.
[37] S.J. Letohay, K. Maštovská, A.R. Lightfield, J. AOAC Int. 88 (2005) 615–629.
[38] D. Mathieu, J. Nony, R. Phan-Tan-Luu, NemrodW (Version 2007_03)L.P.R.A.I. Marseille, France, 2007.
[39] C.A. Andersson, INCA 1.41, Department of Food Science, University of Copenhagen, Denmark. Available at ⟨http://www.models.life.ku.dk/inca⟩ (accessed 30/10/2014).
[40] B.M. Wise, N.B. Gallagher, R. Bro, J.M. Shaver, W. Winding, R.S. Koch, PLS Toolbox 6.0.1, Eigenvector Research Inc., Wenatchee, WA, USA.
[41] MATLAB, version 7.12.0.635 (R2011a), The Mathworks, Inc., Natick, MA, USA.
[42] STATGRAPHICS Centurion XVI Version 16.1.05 (32 bit), Statpoint Technologies, Inc., Herndon, VA, USA, 2010.
[43] L.A. Sarabia, M.C. Ortiz, Trends Anal. Chem. 13 (1994) 1–6.
[44] M.C. Ortiz, L.A. Sarabia, I. García, D. Giménez, E. Meléndez, Anal. Chim. Acta 559 (2006) 124–136.
[45] R. Bro, Crit. Rev. Anal. Chem. 36 (2006) 279–293.
[46] R.B. Cattell, Psychometrika 9 (1944) 267–283.
[47] N.M. Faber, R. Bro, P.K. Hopke, Chemom. Intell. Lab. Syst. 65 (2003) 119–137.
[48] R. Bro, H.A.L. Kiers, J. Chemom. 17 (2003) 274–286.
[49] J.E. Jackson, G.S. Mudholkar, Technometrics 21 (1979) 341–349.
[50] A. Smilde, R. Bro, P. Geladi, Multi-way Analysis, J. Wiley & Sons Ltd., Chichester, 2004.
[51] International Organization for Standardization, ISO 11843, Capability of Detection, Part 1: Terms and Definitions, 1997; and Part 2: Methodology in the Linear Calibration Case, Genève, Switzerland, 2000.
[52] Commission Decision (EC) No 2002/657/EC of 12 August 2002 implementing Council Directive 96/23/EC Concerning the Performance of Analytical Methods and the Interpretation of Results, Off. J. Eur. Commun. L 221:8–36.
[53] J. Inczédy, T. Lengyel, A.M. Ure, A. Gelencsér, A. Hulanicki, IUPAC, Compendium of Analytical Nomenclature, third ed., Baltimore, Port City Press Inc., 2000.
[54] M.C. Ortiz, L.A. Sarabia, A. Herrero, M.S. Sánchez, M.B. Sanz, M.E. Rueda, D. Giménez, M.E. Meléndez, Chemom. Intell. Lab. Syst. 69 (2003) 21–33.
[55] International Organization for Standardization, ISO 5725-2, Accuracy (Trueness and Precision) of Measurement Methods and Results, Part 2: Basic Method for the Determination of Repeatability and Reproducibility of a Standard Measurement Method, Genève, Switzerland, 1994.
[56] L. Rubio, M.C. Ortiz, L.A. Sarabia, Anal. Chim. Acta 820 (2014) 9–22.